Low-Distortion Continuous-Time R-MOSFET-C Filters*

Un-Ku Moon Bang-Sup Song
Department of Electrical and Computer Engineering
University of Illinois, Urbana, IL 61801

ABSTRACT: **R-MOSFET-C or R-MOSFET-R structure, which uses a set of passive resistors and current-steering MOS transistors as a variable resistance element, is proposed to implement low-distortion filter or multiplier in CMOS technology. This proposed technique relies on the linearity of passive resistors and the tunability of current-steering MOS transistors in triode. Placing the nonlinear elements inside feedback loops further reduces distortion in the filter implementation. The experimental results of a self-tuned 22kHz 5th-order Bessel filter confirm the predicted theoretical performance, displaying negligible control voltage feedthrough and -90dB THD with a 2kHz, $4V_{p-p}$ fully-differential signal, in a 5-V system.**

I. Introduction

Among the numerous design techniques to improve linearity and tunability of an active filter, a well known MOSFET-C filter uses the linearized model behavior of an MOS transistor operating in the triode region [1]. In a similar approach, using the MOSFETs in triode in place of resistors, a differentially balanced variable resistance stage has been implemented as a multiplier [2]. In all cases, despite well-behaved tunability, due to mismatch and inherent nonlinear behavior of the MOSFETs, THD of only 40-60dB is feasible with a volt-level signal swing in a single 5-V system. In comparison to the MOSFET-C filter, the R-MOSFET-C filter proposed herein moves this nonlinear variable resistance element inside a feedback loop for a significant distortion reduction. Furthermore, in R-MOSFET-C filter and R-MOSFET-R multiplier, the actual voltage applied to the nonlinear elements is scaled down to operate more closely within their linear range by degenerating the MOSFETs by passive resistors. This degenerated portion is the R-MOSFET stage.

II. Reduction of Distortion in R-MOSFET Stage

An improved variable resistance stage, R-MOSFET, derived from the differentially balanced MOSFET configuration [2], is shown in Fig. 1. In comparison to the conventional voltage controlled resistor, made of four MOSFETs in triode, M1, M2, M3, and M4, the proposed variable resistor operates with a reduced voltage across the active devices and therefore exhibits a lower distortion than the conventional one. The equivalent resistance of the current steering portion is set by the control voltage, V_C. The R-MOSFET stage shown in Fig. 1 has an equivalent resistance of

$$R_{eq} = \frac{1}{G_{1,2}} F \ , \tag{1}$$

where G_i is the transconductance of M_i, defined by

$$G_i = \mu C_{OX} \frac{W}{L} (V_{GSi} - V_{thi}) = K_i (V_{GSi} - V_{thi}) \ . \tag{2}$$

The voltage scale factor, F, is defined by

$$F = \frac{V_i}{V_X} = 1 + 2\bar{G}R \ , \tag{3}$$

if the average conductance of M_1, M_2, M_3 and M_4 is

$$\bar{G} = \frac{(G_{1,2} + G_{4,3})}{2} \ . \tag{4}$$

As F is increased, the distortion is reduced. This effect is identical to the local feedback of an emitter degeneration. The MOSFET devices in this arrangement are no longer used as "resistors" but as current steering devices, operating in the triode region. For the given configuration shown in Fig. 1, when the control voltage, V_C, becomes largely positive, the effective resistance of the R-MOSFET approaches $R + R_{M1,2}$, where $R_{M1,2}$ is the on-resistance of M1 (or M2). M1 and M2 are "on" but M3 and M4 are almost "off." This is the minimum resistance of the variable resistor and sets the limit on one end of the tunable range. As the control voltage becomes largely negative, this in turn sets the limit on the other extreme of this variable resistance element. When implemented as a linearity improved integrator, by replacing

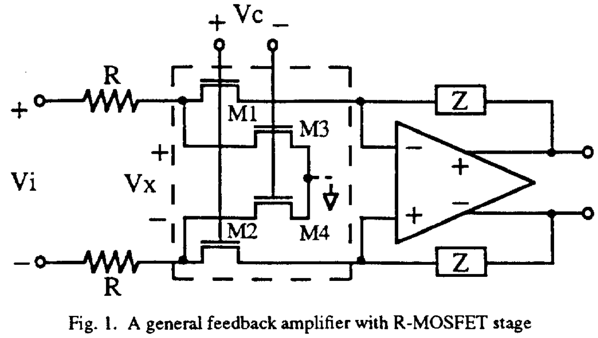

Fig. 1. A general feedback amplifier with R-MOSFET stage

* This work was supported by an NSF grant MIP 90-13166, and partly by Analog Devices and Motorola.

0-7803-1254-6/93$03.00 © 1993 IEEE

the feedback component, Z, with a capacitor, C, the unity gain frequency of this integrator becomes

$$\omega_{unity} = \frac{G_{1,2}}{FC} = \frac{\bar{K}V_{C,n}}{FC}\ , \quad \text{where} \tag{5}$$

$$V_{C,n} = \frac{V_C}{2} + (V_{CM} - V_{th}) \quad \text{and}$$

$$(V_{CM} - V_{th}) = \text{CM overdrive.}$$

Implemented even more closely to the differentially balanced variable resistance stage [2], the R-MOSFET portion of the R-MOSFET-R multiplier shown in Fig. 2 has an equivalent resistance of

$$R_{eq} = \frac{1}{G_{1,2} - G_{3,4}} F\ . \tag{6}$$

This R-MOSFET stage is able to create a negative equivalent resistance according to a negative control voltage, V_C, and is therefore more desirable for a multiplier. The equations (2)-(4) equally apply to this stage. The feedback component, Z, is now a resistor, R. A distinct improvement of linearity is shown in Fig. 3, simulated under a 1% mismatch of MOSFETs and resistors.

Note that the disadvantage of these R-MOSFET variable resistance stages in comparison to simple passive resistors (as in R-C filters) is the reduction of effective dc gain and bandwidth of the operational amplifier. The overall performance error of a filter or a multiplier due to this effective lower gain and bandwidth should be taken into account [3].

III. Distortion Improvement by Feedback Loopgain

A set of feedback loops exists in a filter implementation. Taking these feedback loops into advantage, the use of one current steering element per integrator opens up a new method of placing the nonlinear devices inside the feedback loops. This is to further improve linearity in addition to the passive resistor degeneration previously mentioned in Section II. Consider the first-order filter shown in Fig. 4. The resistor R_2 is fed back from the output of the op amp to the input

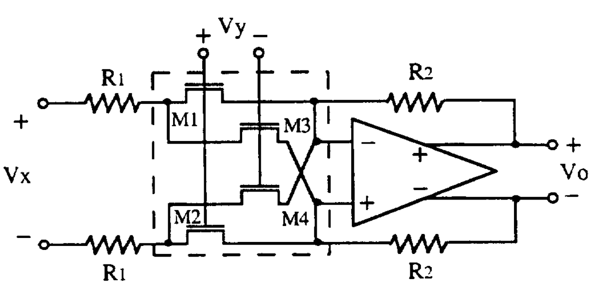

Fig. 2. R-MOSFET-R improved multiplier

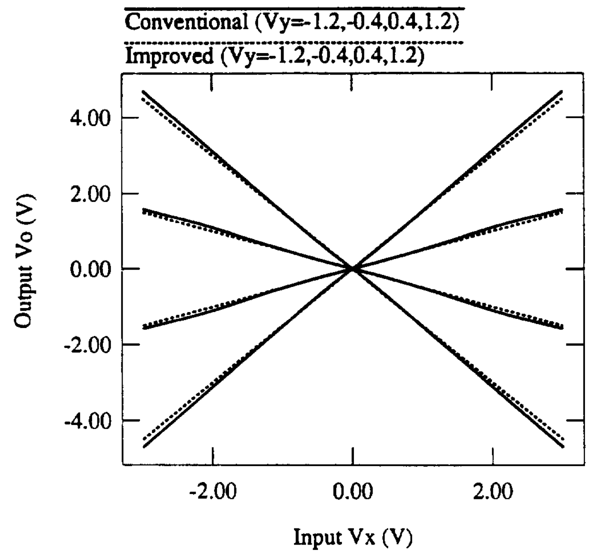

Fig. 3. Bowtie characteristics of a standard 4-quadrant multiplier

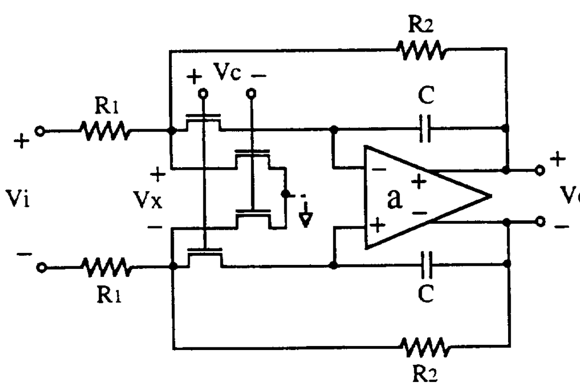

Fig. 4. R-MOSFET-C first-order filter

of the current steering element. As a result, the nonlinear current steering element is placed inside the feedback loop. (Values of R_1 and R_2 must include loading effect.) At low frequencies, the loop gain is $\bar{a}f$, if the transfer function of the MOSFET-C integrator inside the loop is $\bar{a}$ (with same dc gain, a_o, of the op amp) and

$$f \approx \frac{(R\,||\,R_X)}{(R\,||\,R_X) + R} = \frac{1}{F}\ , \quad \text{where} \tag{7}$$

$$R_X = \frac{1}{G_{4,3} + G_{1,2}} = \frac{1}{2G} \quad \text{and} \quad R = R_1 = R_2\ .$$

As a result, MOSFET nonlinearities are reduced by this loop gain within the filter bandwidth. The loop gain decreases as the input frequency passes the dominant pole of the MOSFET-C integrator, and the distortion reduction by the feedback approaches its minimum at the filter passband edge. However, the improvement resulting from the voltage scaling factor, F, stays constant at all frequencies. Taking a closer look into the feedback loop configuration for this low distortion filter, the transfer function of the proposed topology shown in Fig. 4 is

$$-\frac{V_o}{V_i} = \frac{R_2}{R_1}\,\frac{\bar{a}\left(\frac{(R_1||Z_X)}{(R_1||Z_X)+R_2}\right)}{1+\bar{a}\left(\frac{(R_1||Z_X)}{(R_1||Z_X)+R_2}\right)}, \text{ where} \quad (8)$$

$$Z_X = \left(\frac{1}{G_{4,3}}\right)||\left(\frac{1}{G_{1,2}}+\frac{1}{sC(1+a)}\right).$$

Note that

$$f = \frac{(R||Z_X)}{(R||Z_X)+R} \approx \frac{(R||R_X)}{(R||R_X)+R} = \frac{1}{F}, \text{ given} \quad (9)$$

$$R = R_1 = R_2,$$

as mentioned previously. It is clear from the transfer function that the ratio R_2/R_1 is linear, fully relying upon the linearity of the passive resistors, and the right half of the expression is in the format of $T/(1+T)$. This means that all nonlinear functions are inside of a feedback loop where the loopgain, T, that is $\bar{a}[(R_1||Z_X)/((R_1||Z_X)+R_2)]$, reduces distortion within the bandwidth of the filter.

IV. Noise Consideration

In consideration for the dynamic range, equivalent independent noise sources for each of the input resistors, the current-steering element, and the operational amplifier shown in Fig. 1 can be referred to the input for analysis. At low frequencies, the equivalent input referred noise of this stage is given by

$$\frac{\overline{V_{eq}^2}}{\Delta f} = 4KT\left[2R+\left(\frac{R}{R_2}\right)^2 2R_2+\left(\frac{R+R_2}{R_2}\right)^2(2R_1+R_i)\right], \quad (10)$$

where R_i is an equivalent input noise resistance of the op amp. When this expression is analyzed, the noise increases with increasing F and decreasing V_C. It is due to the bypassing of the integrating current in the current steering element that the circuit noise is increased. This noise can be minimized by increasing the on-resistance of the MOSFETs, but a larger on-resistance of the MOSFETs decreases the voltage scale factor, F. Therefore, the noise versus linearity optimization is necessary to minimize the noise contributed by the current steering element. It is found that the distortion of a typical filter implementation can be reduced by 14dB (without the additional reduction by the feedback effect) with less than 3dB increase in the noise power. However, taking into account a quite significant amount of linearity improvement by the feedback loop, a much larger signal swing without distortion can justify the marginal increase in the noise floor.

V. Automatic Tuning

The automatic tuning implemented for the filter takes advantage of the switched-capacitor accuracy in achieving the desired corner frequency [4]. This switched-capacitor tuning method, a mere time constant matching, greatly simplifies the task of automatic tuning. Shown in Fig. 5 is the time constant matching integrator of the linearity improved continuous-time path and the switched-capacitor path. The time constant of the continuous-time path is $R_{eq}C_{int}$ and that of the switched-capacitor path is $C_{int}/f_{clk}C_1$. The mismatch of the two time constants, which simplify as the mismatch of R_{eq} and $1/f_{clk}C$, appears at the output of the integrator. That voltage is then translated to the control voltage of the current steering MOSFETs. R_{eq} is equal to $1/f_{clk}C$ within bounds when the equilibrium is reached. There is an additional circuit block in the final implementation for the CM control voltage. This CM control voltage, V_{CM}, simply maintains the designed voltage scale factor, F. Finally, by placing a large time constant R-C lowpass network in the control loop, equivalently an open loop control is established. This R-C lowpass network is able to sufficiently filter out the clock noises and eliminate control voltage feedthrough.

VI. A Prototype Fifth-Order Bessel Filter

To illustrate the validity of the theory presented, an audio-band (22kHz) fifth-order Bessel filter with a voltage scaling factor, F, varied between 2.5 to 5 was designed and fabricated in a standard 2μ CMOS technology. The filter was designed to be tunable in multiple frequencies and able to tune to the audio-band (22kHz) despite the extremes of process and temperature variations. Fig. 6 is the schematic of the fifth-order Bessel filter using the linearity improvement

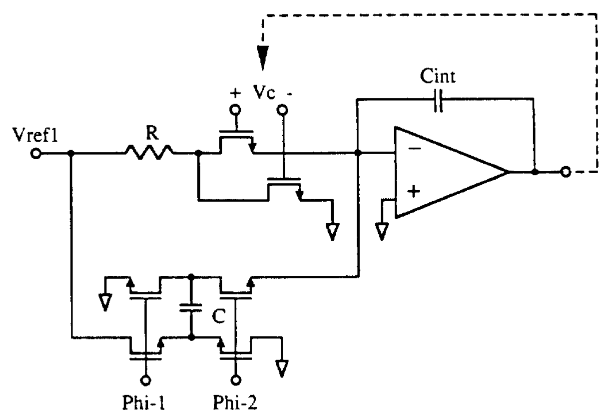

Fig. 5. Automatic tuning using a switched-capacitor reference resistor

technique. The filter coefficients are transformed from the L-C ladder structure to the active R-C structure [5] and are node-voltage scaled. The capacitor sizes are optimized for the dynamic range, given the total capacitance as the constraint, applying a linear programming method [6] while locally linearizing the optimization function with the 1st-order Taylor's approximation. The box with the crossing arrows indicates the current steering portion of the variable resistance stage. Since the Bessel filter poles are low-Q poles, the component values are not critical in this ladder-type implementation. The component values shown in Fig. 6 are mathematically calculated values for reference.

The tuning capability is verified in Fig. 8, in agreement with the simulation. Typical tunability of 10kHz to 35 kHz is observed. Fig. 9 is a plot of the measured THD versus input frequency and the upper boundary of THD simulated with the worstcase combination of parameters, where the input signal is fixed at $4V_{p-p}$ differential. A 1% mismatch of W/L, μ, V_{th0}, and γ for the MOSFETs in the current steering portion is used in simulation. This plot captures the effect of the feedback loop on distortion. As displayed in measurement as well as in simulation, the distortion increases as the input frequency approaches the filter passband edge. The measured THD is better than -90dB at 2kHz.

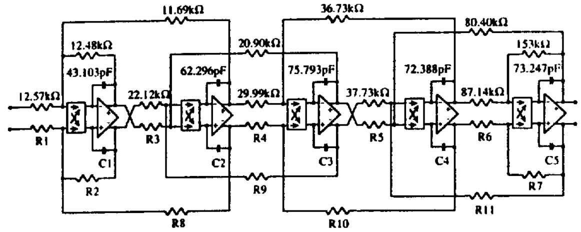

Fig. 6. 22kHz 5th-order Bessel filter

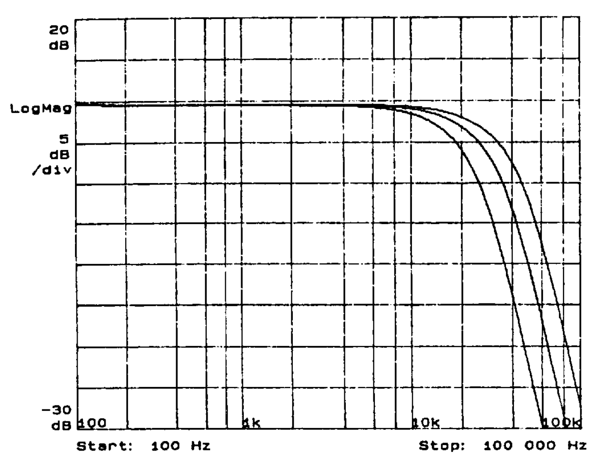

Fig. 8 Frequency response

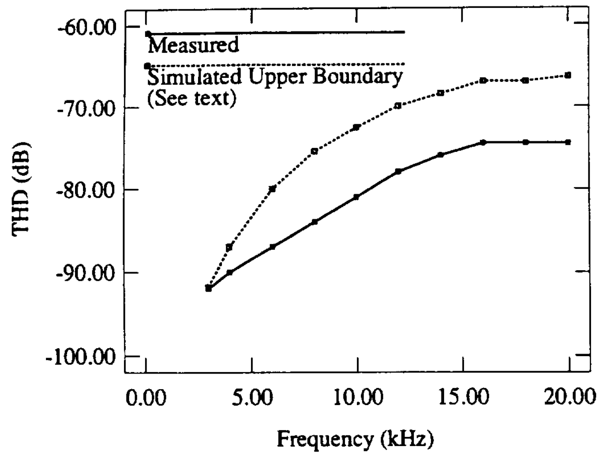

Fig. 9 THD vs. input frequency ($4V_{p-p}$)

VII. CONCLUSIONS

In simulation and in measurement of the prototype filter, the proposed linearity improvement technique, namely R-MOSFET-C filters, has demonstrated an unprecedented performance in linearity, thus establishing the feasibility of no-trim digital audio CMOS filters. This proposed variable resistance stage, R-MOSFET, MOSFETs degenerated by passive resistors, can be implemented as a building block in a variety of applications as demonstrated in the multiplier, integrator, and filter examples.

ACKNOWLEDGEMENT

Authors would like to thank Paul Ferguson and his team, and Seung-Hoon Lee at Analog Devices for providing and helping with simulation and layout tools, and Pat Rakers and Chris Lash at Motorola for testing.

REFERENCES

[1] Y. Tsividis, M. Banu, and J. Khoury, "Continuous-time MOSFET-C filters in VLSI," *IEEE J. Solid-State Circuits*, vol. SC-21, no. 1, pp. 15-29, Feb. 1986.

[2] B. -S. Song, "CMOS RF circuits for data communications applications," *IEEE J. Solid-State Circuits*, vol. SC-21, no. 2, pp. 310-317, April 1986.

[3] K. -L. Lee and R. Meyer, "Low-distortion switched-capacitor filter design techniques," *IEEE J. Solid-State Circuits*, vol. SC-20, no. 6, pp. 1103-1113, Dec. 1985.

[4] T. R. Viswanathan, et al., "Switched-capacitor frequency control loop," *IEEE J. Solid-State Circuits*, vol. SC-17, no. 4, pp. 775-778, Aug. 1982.

[5] A. I. Zverev, *Handbook of Filter Synthesis*, New York: Wiley, 1967.

[6] Gilbert Strang, *Linear Algebra and Its Applications*, Third Edition, pp. 405-410, San Diego: HBJ, 1988.